BIOMIMETICS

Bioinspired underwater legged robot for seabed exploration with low environmental disturbance

G. Picardi[1,2], M. Chellapurath[1,2,3], S. Iacoponi[1,2], S. Stefanni[3], C. Laschi[1,2], M. Calisti[1,2]*

Robots have the potential to assist and complement humans in the study and exploration of extreme and hostile environments. For example, valuable scientific data have been collected with the aid of propeller-driven autonomous and remotely operated vehicles in underwater operations. However, because of their nature as swimmers, such robots are limited when closer interaction with the environment is required. Here, we report a bioinspired underwater legged robot, called SILVER2, that implements locomotion modalities inspired by benthic animals (organisms that harness the interaction with the seabed to move; for example, octopi and crabs). Our robot can traverse irregular terrains, interact delicately with the environment, approach targets safely and precisely, and hold position passively and silently. The capabilities of our robot were validated through a series of field missions in real sea conditions in a depth range between 0.5 and 12 meters.

INTRODUCTION

The continued development of technologies for robotics, combined with the growing ambition of roboticists, will enable robots to venture out of laboratories and production lines into unstructured and dynamic environments to carry out all sorts of useful tasks. However, a wide range of interdisciplinary cross-fertilizations from the fields of biology, chemistry, neurosciences, and social sciences are required to sustain advances in robotics (*1*).

The study of nature and the attempt to abstract its fundamental principles can lead to a bioinspired approach to the design of robots (*2*, *3*) and potentially increase their performance or enable previously unexplored capabilities (*4*). For example, the successful application of a bioinspired approach led to the development of highly performing mobile machines (*5*–*7*), a novel manipulation system that can conform to its environment (*8*), and strong adhesive pads that can attach to a wide variety of surfaces (*9*). At the same time, robotics can be used to study nature. Robots can be invaluable tools to collect scientific data that would be otherwise inaccessible, because of their ability to withstand harsh environments, reach remote places, and operate autonomously. Tasks such as the autonomous tracking of radio-tagged birds with drones (*10*) or adaptive sampling of phytoplankton with autonomous underwater vehicles (AUVs) (*11*) represent important contributions of robotics to conservation and ecology. Moreover, space and ocean exploration (*12*–*14*), which holds potential to answer fundamental questions on the origin of the universe, could not be carried out without robotic tools due to the extreme conditions of the environment (*15*).

Up to now, most of the robots used to collect scientific data belong to more traditional classes of vehicles, such as thruster-driven drones, AUVs, or wheeled rovers. Most biomimetic robots are built to mimic the morphology of an animal and used to validate scientific hypothesis (*16*, *17*). An exception to this trend is represented by a remotely operated soft fish (*18*), which, because of its bioinspired locomotion, allows close-up observation of marine life without the disturbances introduced by thrusters.

The ocean is essential for life on our planet; it plays a critical role in climate regulation and balancing various ecosystems (*19*, *20*). It is also home to countless biological species and diverse environments (*21*). At the same time, the ocean represents the main global transportation channel (*22*); it is an indispensable source of energy, which can be obtained through the conversion of waves (*23*) and wind in offshore farms (*24*), as well as numerous underwater oil and gas reservoirs (*25*); and fish is a fundamental source of protein for people all over the world (*26*). Despite its vital importance, the ocean is still underexplored due to the incredibly harsh conditions that prevent its exploration by conventional means. Ocean exploration using underwater robotics, such as AUVs or remotely operated vehicles (ROVs), is becoming increasingly popular (*27*) because it enables safe exploration in extreme environments for an extended period of time. Nowadays, underwater robots are used in several application fields ranging from the oil and gas (*28*) and fish farming industries (*29*) to archeology (*30*), search and rescue (*31*), and defense (*32*). Underwater robotics also play an important role in several fields of scientific research. Successful applications of underwater robots in scientific tasks include the mapping of composition and environmental parameters of water over space and time (*33*); the characterization of the seabed in terms of bathymetry (*34*), morphology, and composition (*35*); the study of glacial regions and icebergs (*13*, *36*); the observation of biological species in their environment (*11*, *18*); the collection of biological and geological samples (*37*); the search for life in the deep (*38*, *39*); and contributing to protect the environment against pollution (*40*).

Regardless of the application, most underwater robots are pelagic—that is, they move in the water column by mean of thrusters—and for this reason, they present intrinsic limitations when it comes to interacting with the environment. The most common approach consists of hovering above a certain position and performing station keeping and manipulation algorithms at the same time (*27*, *41*). Besides being computationally heavy, this approach suffers from the disturbance of currents (*42*) and is subject to many modeling and identification uncertainties. To simplify the interaction with the environment, it is often preferred to land. However, not all seabed types are favorable to landing, and the turbulence generated by thrusters could displace debris and consequently reduce the visibility or alter the samples that should be collected. When accurate inspection

[1]The BioRobotics Institute, Scuola Superiore Sant'Anna, Pisa, Italy. [2]Department of Excellence in Robotics & AI, Scuola Superiore Sant'Anna, Pisa, Italy. [3]Stazione Zoologica Anton Dohrn, Napoli, Italy.
*Corresponding author. Email: marcello.calisti@santannapisa.it

and sampling tasks are required, an improved interaction may be achieved by benthic vehicles, for instance, vehicles that move directly on the seabed. For this reason, heavy tracked or wheeled vehicles, namely, crawlers, have been proposed in applications ranging from long-time monitoring of the seabed over transects (*39*) to deep-sea bacteria sampling (*43*). Unfortunately, crawlers suffer from uneven or slippery terrains and fissures in the ground; they may substantially modify the substrate on which they move (*9*); low gravity reduces their mobility (*44*); and they require large research vessels to be operated. An alternative approach could be to use legs to ensure safe contact, agility, and static stability in ground locomotion. The newly born category of underwater legged robots (ULRs) has the potential to exploit such unique features to increase the exploration and interaction capabilities of existing underwater vehicles.

The idea of harnessing the benefits of legged locomotion in underwater operations started in the late 1990s; however, since then, just a few prototypes have been built and tested. The first ULR concepts ever developed were hexapod vehicles built with the aim of improving ground measurements during underwater construction duties [Aquarobot (*45*)] and searching and possibly disabling mines in the surf zone [Ariel and Ursula (*46*)]. More recently, arthropods became a source of inspiration for roboticists who developed a biomimetic vehicle to investigate the behavior and control strategy used by lobsters (*17*), as well as a car-sized hexapod robot designed to reject the disturbance of currents by exploiting the orientation of its shell, like crabs and lobsters [Crabster (*47*)]. Regardless of the size or envisioned application, these prototypes do not present compliant components in their legs and resort to a so-called static locomotion strategy, which is based on the inverse kinematic model of the robot and for which stability is obtained by keeping the horizontal projection of the center of mass (CoM) within the support polygon defined by the legs in contact with the ground (*48*). Although being capable of precise movements and individual limb positioning, in practice static legged locomotion appears inadequate for unstructured environments because all the burden of adaptation is left on the controller, and a very high degree of situation awareness (e.g., the construction of an environment map) is required.

In the terrestrial environment, one way of overcoming such limitations was looking at the fundamentals of legged locomotion as observed in animals (*49*) and described by low-order mathematical models (*50*, *51*). This approach stimulated the use of compliant elements in the development of robotic hardware (*52*) and the exploitation of the natural dynamics of the system in control (*53*) and led to the development of very agile machines capable of easily negotiating irregular terrains and reach unprecedented performance (*54*–*56*). In particular, the ability of transitioning from terrestrial to underwater environment was demonstrated by AQUA (*57*) and RoboTerp (*58*), which were able to switch from different terrestrial gaits on the shore to swimming through a phase of legged locomotion in very shallow water by resorting to compliant paddle-like limbs.

A path similar to the one followed by terrestrial legged robotics in the underwater environment was envisioned by our group and is summarized in Fig. 1. The observation of the *Octopus vulgaris* inspired the development of poseiDRONE, a robotic prototype featuring soft silicone limbs used to abstract the dynamics of the benthic locomotion (*59*). Further biological inspiration came from the observation of crabs and the description of their underwater punting gait characterized by backward-directed pushing actions alternated with noncontact phases (*60*). With the aim of explaining the fundamentals of benthic legged locomotion, an extension of the spring-loaded inverted pendulum (SLIP) template (*50*), including the contributions of the underwater environment (drag, buoyancy, and added mass) and a linear actuator, was introduced (*61*). Such a model, namely, underwater SLIP (U-SLIP), is characterized by very attractive autostabilizing properties strongly connected with its leg compliance and morphological features (*62*) and was used as the base for the development of a new class of single and multi-legged underwater robots based on rigid legs with serial elastic actuators (SEAs). First, two single-legged prototypes were developed to validate the U-SLIP model (*63*) and study the effects of different morphologies on the locomotion features and stability (*64*). Later, a quadruped vehicle with linear legs called SILVER (Seabed Interaction Legged Vehicle for Exploration and Research) was built to enable static gaits and demonstrate how to anchor the U-SLIP model to multi-legged locomotion (*65*) even without the feedback from contact sensors.

Here, building on the experience of SILVER, we developed SILVER2, which implements the U-SLIP model on a six-legged underwater robot with articulated legs and harnesses bioinspired principles as actual advantages for field missions. Instead of refining traditional pelagic underwater robots to adapt them to the exploration and interaction with the seabed, here, we present a different concept: a benthic legged robot that moves directly on the seabed. The robot embodies a bioinspired locomotion principle that enables the ability of traversing irregular terrains and enhances the versatility of the class of ULRs. SILVER2 features an electronic subsystem that includes an inertial navigation system, contact sensors, a pressure sensor and two cameras, and six segmented legs with SEAs in the knee joints. In the framework of underwater robotics, the unique combination of compliance with segmented legs grants SILVER2 a good workspace, mobility, and static stability, making it adequately equipped to complement humans or traditional vehicles in underwater operations in the benthic environment. The bottom part of the robot is available to host additional sensors, instrumentations, or manipulators: In the configuration shown in this work, the robot is equipped with a sand-sampling device (Fig. 2).

We demonstrate advantages of underwater legged vehicles in real-world scenarios (reported data were taken from 10 missions in different locations and time in real sea conditions in a depth range between 0.5 and 12 m). Our ULR is capable of (i) terrain traversing, (ii) precise positioning, (iii) operating with low environment disturbances, and (iv) low noise pollution, obtained with simple control and low energy consumption.

RESULTS

In the design of SILVER2 (Fig. 2), we pursued a bioinspired approach based on the observation of locomotion of benthic animals and on a low-order mathematical model capable of catching the fundamentals of the dynamics of running in the underwater environment (punting). The damping effect of hydrodynamic drag, the reduced weight due to buoyancy, the stabilizing momentum generated by positioning the center of buoyancy (CoB) above the CoM, and the compliancy of the legs markedly reduced the risk of falling even in perturbed conditions. Moreover, the use of legs and static gaits based on the inverted kinematics of the robot allowed precise motion when required. Locomotion modalities available to the robot were

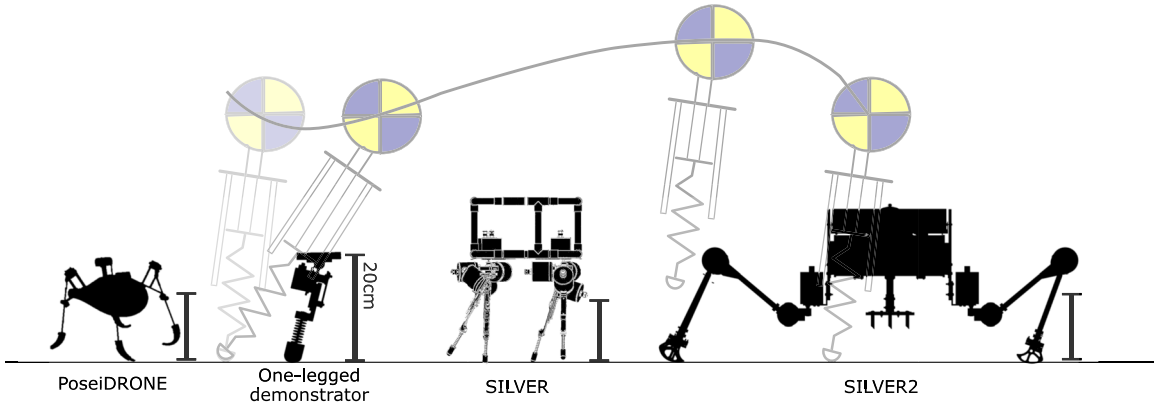

Fig. 1. The evolution line of ULRs that generated SILVER2. The first prototype to study dynamic benthic locomotion was poseiDRONE. Later, an abstraction effort lead to the introduction of the U-SLIP model (on the background) and the consequent development of single-legged hopping demonstrators, the four-legged SILVER, and eventually the hexapod SILVER2. Approximate dimensions are indicated by scale bars beside each robot.

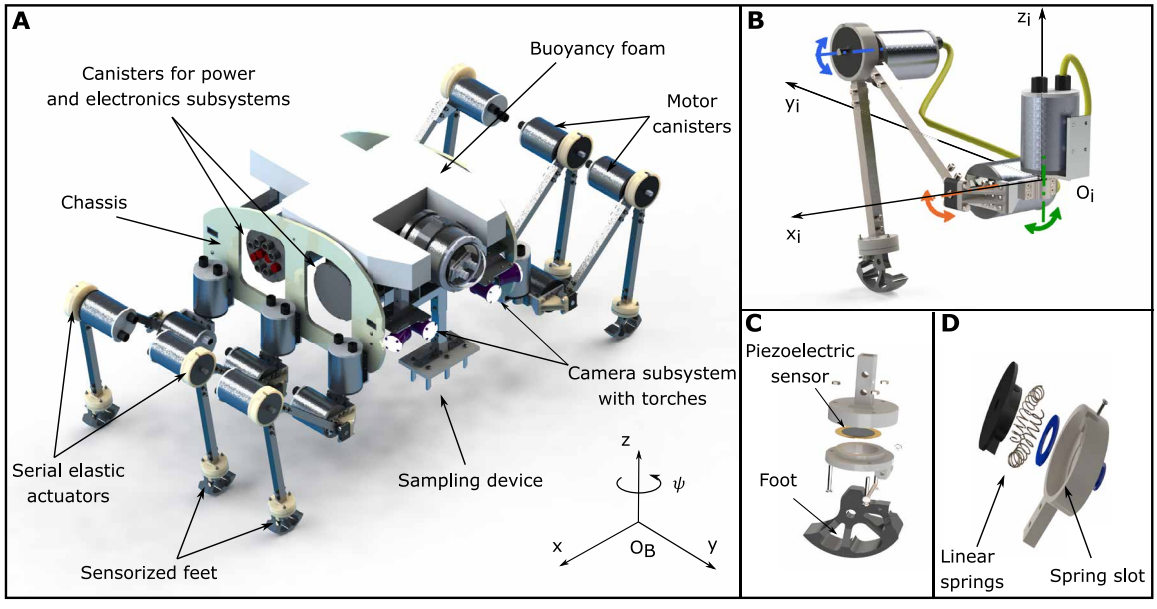

Fig. 2. CAD drawings of SILVER2. (**A**) A CAD drawing of SILVER2 highlighting all main components and the body frame. The center of the body frame O_B is in the geometric center of the robot. The body of the robot is about 35 cm by 60 cm by 70 cm and weighs 22 kg including legs. (**B**) Segmented leg of SILVER2 with three DOFs, namely, coxa (green), femur (red), and tibia (blue) joints. Legs' length from coxa joint to foot tip is about 60 cm. The leg frame of leg *i* is centered in O_i located on the vertical axis defined by the coxa joints, at the same height of the femur joint axis. The coxa joint allows rotations of the whole leg around the *z* axis. The femur and tibia joints define the leg position in the vertical plane set by the coxa angle. (**C**) The distal part of the leg is hinged to an aluminum foot that presses on a piezoelectric sensor to sense touchdown and takeoff with the ground. (**D**) The tibia joint is equipped with a SEA implemented with two linear springs ($k = 10$ kN/m), which enables the hopping locomotion.

hopping, either sideways or rotating in place, and omnidirectional walking [additional details available in the Supplementary Materials and (*65*)]. Predefined poses were also implemented to stand still or to lay onto the seabed to collect sand with a sampling device. In all experiments, the robot was equipped with buoyant elements to achieve an underwater weight of 150 g (1.47 N).

Typical profiles of vertical acceleration (a_z), absorbed current (c), and vertical position (z) for the actions of hopping, walking, and holding position and sampling the sediment are shown in Fig. 3 (D to F). Acceleration data have been filtered by the inertial measurement unit (BNO055) to align the z axis with gravity and subtract its contribution. The hopping gait (Fig. 3, A and D) was based on the U-SLIP model and consists of elongating all legs to push the sediment anytime a foot gets in contact with the ground (punting phases), thus causing the storage of elastic energy in the springs placed in the knees. Once the elastic force exceeds the other contributions, the robot hops off the ground and follows a ballistic trajectory (swimming phases), during which the legs are brought back in position until it touches the ground again. Depending on the relative positions of the legs during the pushing actions, the hopping gait can result in locomotion along a desired axis or in a rotation in place; however, the observed vertical dynamics is the same in both cases. The profile of a_z presents positive peaks corresponding to the instant when the robot touches the ground (touchdown event) and

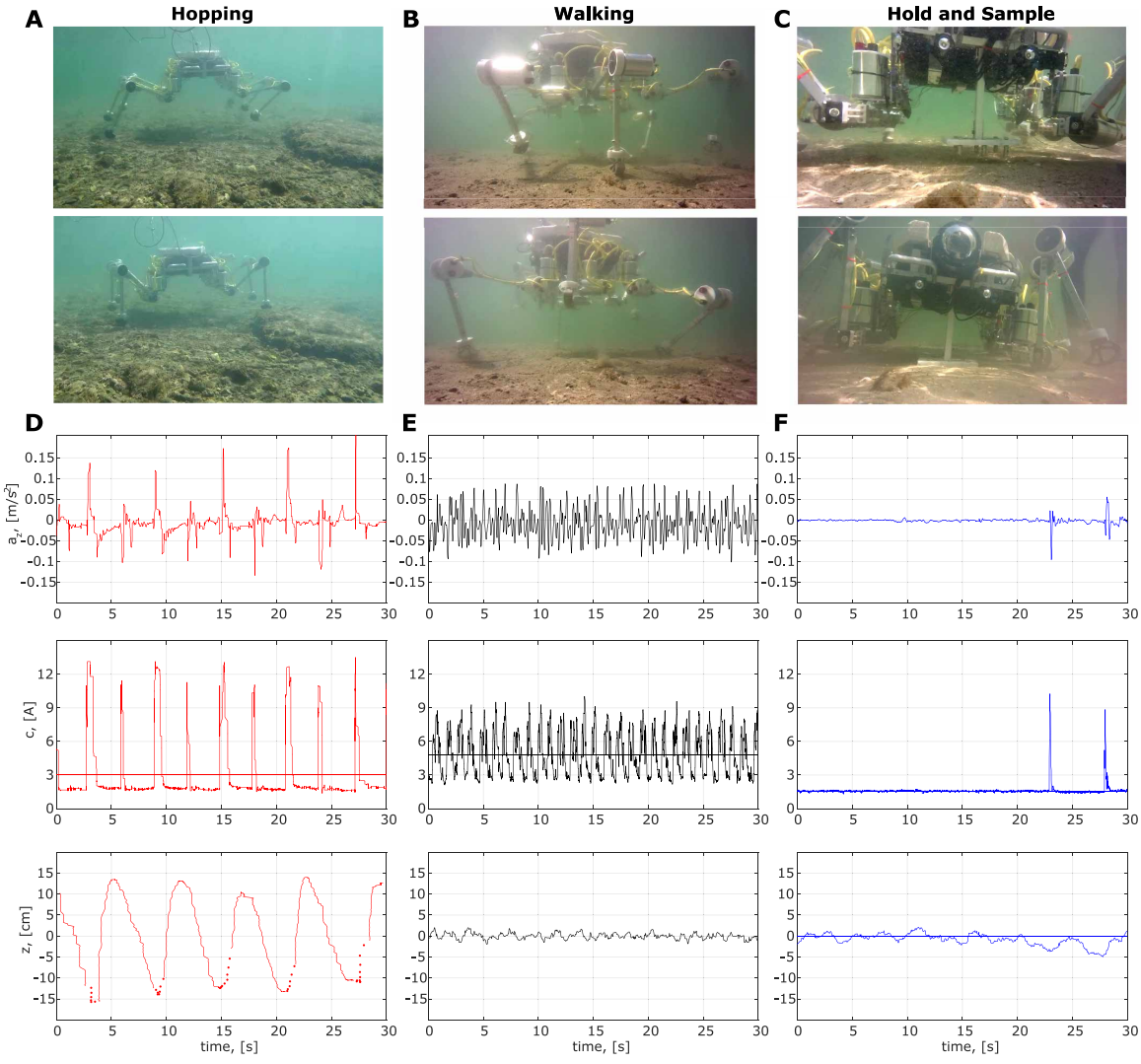

Fig. 3. Examples of actions of SILVER2. (**A** to **C**) Still frames of sideways hopping, omnidirectional walking, and holding position and sampling. (**D** to **F**) Typical profiles of vertical acceleration a_z, current absorption c, and vertical position z for 30 s of hopping, walking, and station keeping and sampling. Solid horizontal lines indicate mean values for current profiles and vertical position in the holding position. Vertical position is offset to zero to show the fluctuations around the mean value. In the vertical position z for the hopping, the dotted line represents the moments when the robot is in contact with the ground (punting phases), whereas the solid lines indicate the trajectory followed by the robot when it was not in contact with the ground (swimming phases).

pushes. The pushing action, represented by a dotted line in z, corresponds to the phase of maximal energy expenditure as shown by the profile of c. During the swimming phase, instead, some energy is spent to take the legs back in position, and a corresponding negative peak can be observed in a_z due to the inertia of the legs themselves.

The walking gait (Fig. 3, B and E) is based on the kinematic model of the robot's legs as in (*48*) and consists of controlling each joint in position so that each leg follows a preprogrammed trajectory and the robot globally translates. Collected data, particularly a_z and c, present higher frequency profiles with lower peaks associated to stance and swing phases of all legs. The mean current absorbed is generally higher, and the vertical position z is kept almost constant throughout the gait.

Last, station keeping (or position holding) simply consists of keeping all motors in position, whereas the sampling action consists in a coordinated action of all legs to lower the posture and shovel the sediment with the sampling system and go back to the station-keeping condition. During station keeping (from second 0 to 20 in Fig. 3F), a_z is almost null, the only energy is drained by the on-board electronics, and the vertical position data slightly oscillate. Being derived from pressure data with a static conversion, the z plot during station keeping can provide an estimation of the waves' height.

On the other hand, the sampling action (from second 20 to 30 in Fig. 3F) is characterized by a negative peak followed by a positive peak in a_z, respectively corresponding to the contact and the detachment of the sampling system with the ground. The current has two peaks in the same time instants, while the vertical position is lower than the mean value observed during station keeping.

A total of 10 sea missions, with an approximate duration of 2 hours each, were performed over different grounds, grossly classified as rock and slit (R), flat sand (S), sand dunes (D), and mud and seaweed (M). Two preliminary tests were carried out in a swimming

pool (P). The robot demonstrated consistent and repeatable behavior during all missions performed, as shown by Table 1, which reports the mean and SD of statistics observed during multiple trials for the different actions. The same trends presented in Fig. 3 were observable across all kinds of terrains tested.

Locomotion on uneven terrain

SILVER2 was capable of traversing all kinds of terrains tested without any previous knowledge of the ground. Examples of tested grounds are shown in Figs. 4 (D to F) and 5B.

Notwithstanding the great variability in the environmental conditions in which the robot was tested, the main locomotion features extracted from the onboard sensors and reported in Table 1 depict a consistent hopping behavior on all kinds of terrains. In particular, the robot moved with a very steady mean frequency $\bar{f}$ = 0.17 Hz regardless of hopping sideways or rotating. The vertical dynamics was generally characterized by an average displacement Δz of around 12 cm with acceleration peaks (0.21 m/s^2), substantially higher with respect to walking. The variability in Δz can be explained by the presence of slopes and terrain irregularities such as rocks or local depressions, which might have anticipated or delayed the touchdown event at any step, as shown by the trial reported in Fig. 4G. The current absorbed was very consistent across trials, with higher mean $\bar{c}$ and peaks max(c) generally correlating with higher vertical displacements. In comparison with walking, the mean absorbed current was substantially lower but presented higher peaks due to impacts with the ground at touchdown (see Table 1). With an average current value of 2.54 A, sideways hopping was the gait reporting the lowest energy consumption, followed by hopping rotating (2.98 A) and eventually walking (3.7 A). However, the peak current was lowest in walking (8.72 A), followed by hopping sideways (12.9 A) and rotating (15.52 A). A gross estimation of the energetic autonomy, with the on-board battery of the robot (12-V, 25,000-mA lithium battery), is about 10 hours for hopping and 7 hours for walking.

All tested ground, but the pool (P) presented high-frequency disturbances (i.e., rocks and asperities) and low-frequency disturbances, such as a small decline of the ground, which were negotiated during the different actions and reported in the Slope column in Table 1. The ratio between the Slope and the estimation of distance traveled (when available) revealed that the robot successfully negotiated slopes of about 15%. A substantial variability in the mean turning rate $\bar{\psi}$ was observed for both sideways and rotating hopping. In the case of sideways hopping, as opposed to rotating, $\bar{\psi}$ is an undesired deviation from the straight trajectory, and thus, a higher value corresponds to a poorer performance. For both types of hopping, the worst performance was observed on the mixed terrain (R) and the best on flat sand (S). This outcome was expected because the rocks and irregularities of the mixed terrain were likely to affect the consistency in the pushing directions.

Rocks with a maximum height of about 7 cm were also negotiated by the hopping locomotion (Fig. 3A). This contributed to undesired rotation but confirmed the reliability of the robot over complex ground. Vertical displacement and forward speed are inversely correlated in U-SLIP (*62*) and in our robot; with the pushing strategy used in this work, we ensured all-terrain hopping locomotion because of a good vertical excursion but with a payback in speed, which was estimated with trials in a premeasured stretch of sea (Fig. 4A) as 8.7 cm/s on average, with a maximum speed of 12 cm/s and a minimum of 4.3 cm/s. Walking locomotion was more consistent, with an average walking speed of about 5.45 cm/s, a maximum of 5.8 cm/s,

Table 1. Relevant statistics from on-board sensors for each gait and action performed by the robot on all tested terrains. Terrain labeled as R corresponds to rocks and silt, S corresponds to flat sand, D corresponds to sand dunes, M corresponds to mud and seaweed, and P corresponds to flat tiles in a swimming pool. The statistics displayed are mean and maximum current absorbed [$\bar{c}$ and max(c)], maximum vertical acceleration max(a_z), slope over a trial, mean turning rate $\bar{\psi}$, mean hopping frequency $\bar{f}$, and mean vertical displacement Δz. Standard deviations are reported between parentheses. Dashes indicate unavailable data. Statistics for hopping and walking are presented grouped per terrain type as well as aggregate for all kinds of terrain traversed. Hopping is further differentiated into sideways and rotating.

	Terrain	$\bar{c}$ (A)	Max(c) (A)	Max(a_z) (m/s^2)	Slope (cm)	$\bar{\psi}$ (deg/s)	$\bar{f}$ (Hz)	Δz (cm)
Hopping	All	2.69 (0.52)	13.81 (1.98)	0.21 (0.06)	8.56 (10.40)	–	0.17 (0.01)	12.3 (8.01)
Sideways	All	2.54 (0.43)	12.9 (1.59)	0.20 (0.08)	7.83 (11.31)	0.54 (0.69)	0.17 (0.01)	9.69 (4.92)
	R	2.36 (0.37)	12.66 (1.79)	0.21 (0.10)	8.62 (13.68)	0.72 (0.79)	0.16 (0.02)	8.37 (2.98)
	S	3.15 (0.09)	13.66 (0.63)	0.22 (0.04)	10.89 (1.38)	0.11 (0.03)	0.16 (0.00)	5.81 (0.16)
	D	2.74 (0.29)	13.22 (1.48)	0.19 (0.01)	3.15 (0.66)	0.21 (0.04)	0.17 (0.01)	16.64 (5.75)
Rotating	All	2.98 (0.60)	15.52 (1.45)	0.21 (0.03)	9.93 (9.38)	1.42 (1.38)	0.17 (0.01)	17.2 (10.5)
	R	2.05 (–)	14.92 (–)	0.21 (–)	1.97 (–)	0.68 (–)	0.16 (–)	15.20 (–)
	S	2.98 (0.48)	15.90 (1.34)	0.20 (0.03)	12.02 (10.96)	1.87 (1.60)	0.17 (0.01)	14.41 (9.64)
	D	3.44 (0.52)	14.89 (2.36)	0.23 (0.01)	8.69 (6.86)	0.69 (0.67)	0.18 (0.00)	27.90 (9.19)
Walking	All	3.70 (0.61)	8.72 (1.92)	0.10 (0.06)	2.87 (3.27)	0.26 (0.14)	–	3.52 (0.87)
	R	3.90 (0.57)	9.74 (0.55)	0.12 (0.05)	3.78 (3.31)	0.24 (0.16)	–	2.30 (2.62)
	M	3.09 (–)	9.37 (–)	0.10 (–)	11.21 (–)	0.27 (–)	–	2.18 (–)
	P	3.10 (0.16)	5.67 (0.59)	0.04 (0.01)	0.12 (0.09)	0.28 (0.14)	–	2.40 (0.19)
Sampling	All	1.80 (1.20)	9.55 (0.99)	0.08 (0.03)	–	–	–	–
Station keeping	All	1.56 (0.06)	–	0.005 (0.001)	–	–	–	1.31 (1.82)

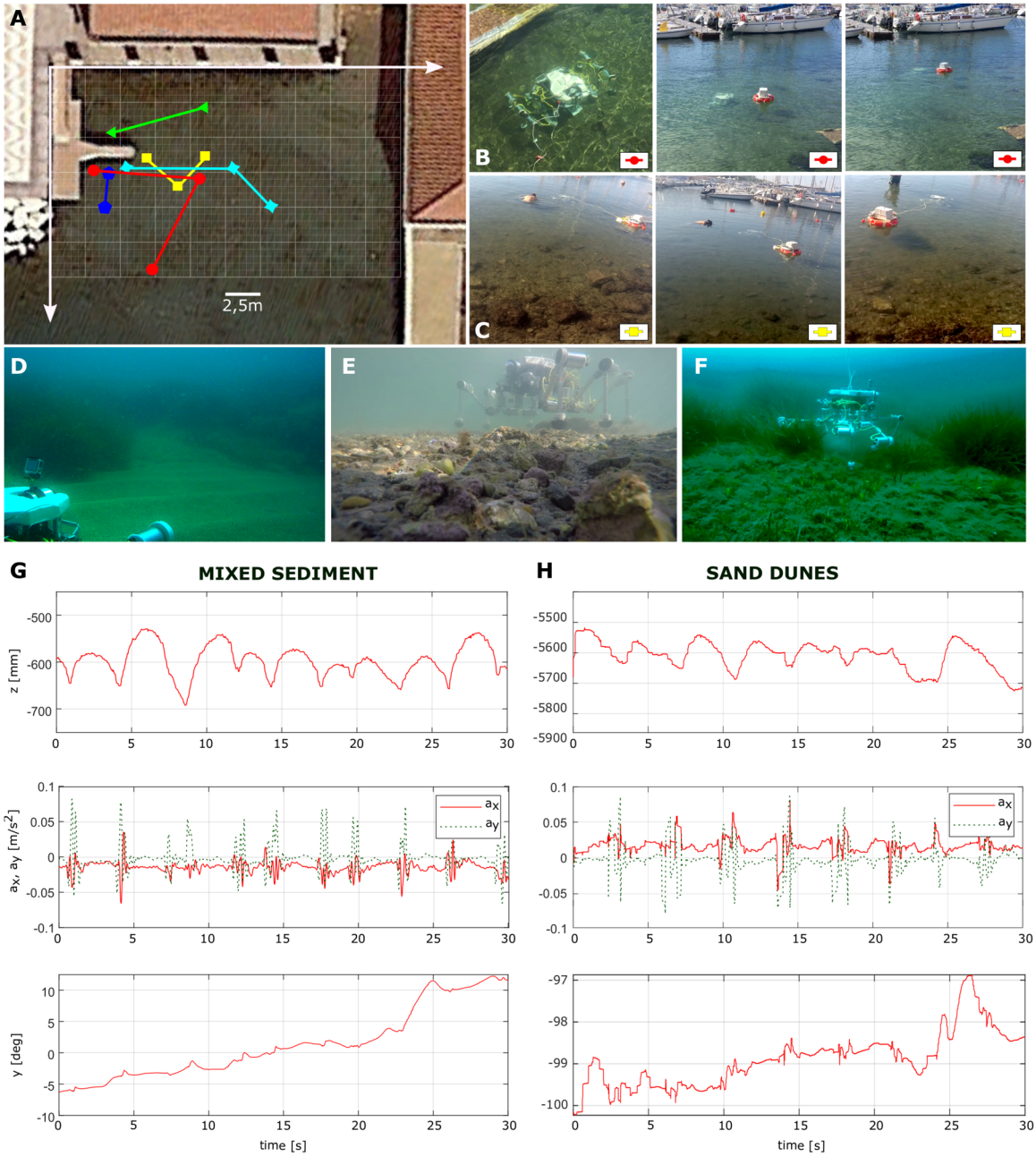

Fig. 4. Hopping locomotion on different types of terrain. (**A**) Body of shallow water (R) with distance references to reconstruct horizontal trajectories and distance traveled by the robot. (**B** and **C**) Still frames of two reconstructed trajectories. (**D**) Sand dunes. (**E**) Mixed sediment with silt and rocks. (**F**) Mud and seaweed. (**G** and **H**) Plots of vertical dynamics, accelerations, and yaw angle for mixed sediment with rocks and sand dune, respectively.

and a minimum of 4.91 cm/s. The cost of transportation (CoT) for the two locomotion strategies can be evaluated as P/mgv, where v is the velocity and $P = V_{cc}\bar{c}$ is the power in input to the system, which is calculated as the product of $V_{cc} = 12V$ and the mean current absorbed $\bar{c}$. Using the average velocities reported above and the values of $\bar{c}$ reported in Table 1, we respectively found a CoT of 1.62 and 3.77 for hopping and walking, respectively.

Interaction with the seabed

The peculiar locomotion modalities used by SILVER2 highlighted two benefits of legged interaction with the seabed: On one side, a localized and low value of force is exerted to the environment, thus reducing the influence of the robot over the environment; on the other side, no disturbances were induced on volatile particles or other elements (mud, weed, etc.) that could impair observation capabilities.

The footprint reported in Fig. 5A demonstrated the discrete nature of the legged locomotion, which has to be compared with the groove produced by tracks in other seabed vehicles (*39*). During the sea missions of SILVER, small circular footprints could be observed in all the gaits performed on sand, with a gait-dependent depth of a few centimeters (about 1 to 2 cm). Walking gait resulted in the shallowest footprints, whereas sideways and rotating hopping had similar

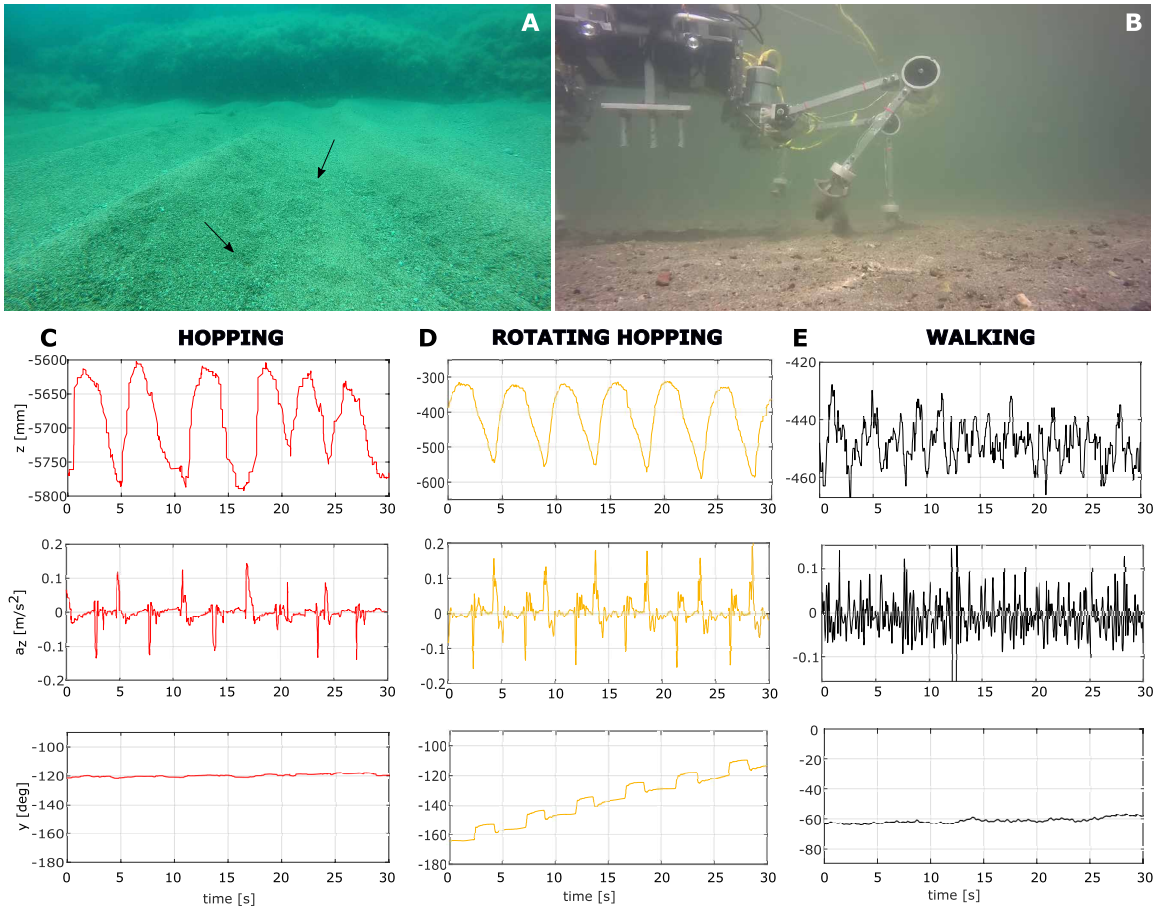

Fig. 5. Interaction of the robot with the substrate. (**A**) Footprints on sand, highlighted by arrows. (**B**) Small clouds of sand raised in worst conditions. Vertical position, acceleration, and yaw, respectively, during sideways hopping (**C**), rotating hopping (**D**), and walking (**E**).

outcomes. On the rocky and muddy substrate, we found no evidence of observable footprints.

The accelerations recorded during the different gaits provided a quantitative measurement of the force exerted to the environment. The vertical acceleration a_z with respect to hopping and walking gaits is reported in Fig. 5 (C to E) and Table 1. The first two locomotion strategies showed discontinuous and periodic vertical accelerations with a maximum of about 0.2 m/s^2 (Table 1), which, including the underwater weight of the robot (1.47 N), corresponds to an overall force of about 3.43 N (0.57 N each foot). In the walking gait, it was difficult to distinguish a periodic behavior from the acceleration signals: Although the a_z had a higher number of peaks, the maximum value is lower (Fig. 5, C to E, and Table 1), and the overall force exerted to the ground during locomotion, including the weight of the robot, is about 2.45 N (0.41 N each foot). We observed no notable differences with respect to the ground, with the SEA acting as mechanical absorbers when sturdy ground (typically big rocks) affected the leg.

Either in the sandy substrate or in the muddy one, the debris raised by SILVER during locomotion was very small if not absent at all. Hopping locomotion has high peaks in the acceleration at touchdown, which, however, raised very small clouds of sand during liftoff. An even gentler interaction can be achieved by resorting to the walking gait, which does not push onto the ground and where acceleration peaks are smaller. In this case, the controlled and slow movements of the leg ensure the minimum amount of sand displaced from the seabed. The worst case for sand displacement happened when the particles were accidentally trapped into the cuts of the foot (Fig. 5B), a trivial drawback that can be easily fixed by substituting the modular foot.

Target approaching

The approaching procedure performed during sea operations is reported in Fig. 6. The pilot led the robot near the target with the dynamic hopping gait, which is suitable to transverse irregular terrain but does not allow full control of the vehicle by the operator because of the non-actuated swimming phases (Fig. 6A). Subsequently, the robot rotated in place to reach an approximate orthogonal orientation, and last, a walking gait was set up to get close to the target and refine positioning (Fig. 6B). Rotation and walking were used more than once, if required. Refinement operations (Fig. 6C) were visually driven by the pilot through the camera feedback on the user interface, with the goal of getting as close as possible to the target (Fig. 6G) or reaching an orthogonal orientation with the target in the middle of the frame (Fig. 6F).

Walking speed was set to 5 cm/s, and the recorded one was slightly lower. With this value, it is easy to stop the robot in the desired position. It is worth mentioning that underwater currents

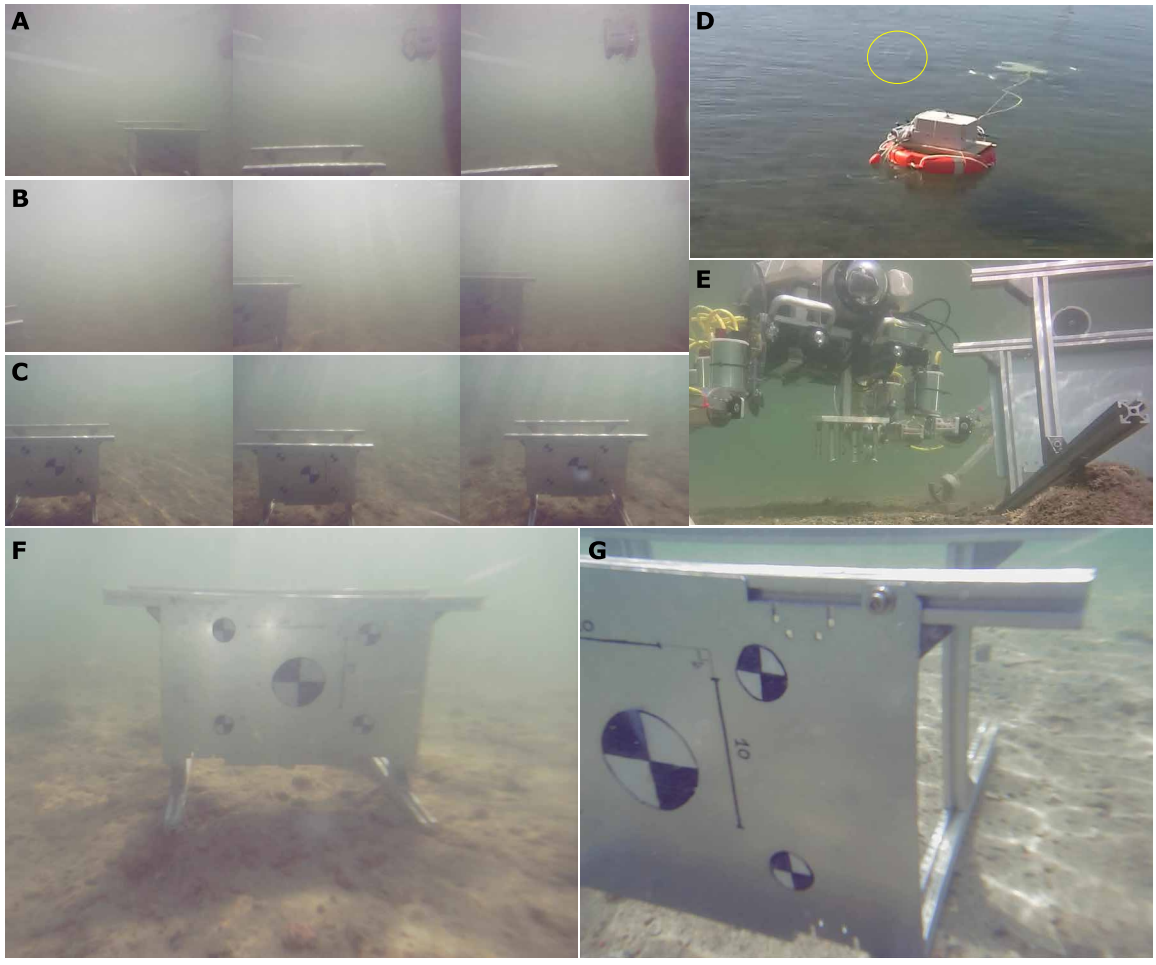

Fig. 6. Approaching procedure from the robot's point of view. (**A** to **C**) The proximity of the target is reached with sideways hopping gait, and then, position and orientation are refined to obtain the desired pose. (**F**) Eventually, legs are placed in a specific stance to optimize visibility. (**D** and **E**) Views from outside camera and on-board cameras are reported, where the target is within the yellow circle. (**G**) Lines smaller than 1 mm are visible, because of the close and stable position of the robot with respect to the target.

and wave disturbances did not influence the speed or the control, although the tests were performed in shallow water conditions where waves have relevant influence. In all the experiments, the robot never affected the target and reached a minimum distance of less than 10 cm (measured as distance between camera dome and target). Even with the relatively small resolution of our on-board cameras for visual feedback (800 pixels by 600 pixels), by getting really close to the target, we were able to distinguish small calibration lines on the frontal side of the target.

Passive station keeping

Station keeping is a very important task for underwater robots with critical implications for manipulation, sampling, data acquisition, and energy efficiency. Currently, this is an open challenge for traditional ROVs, with envisioned solutions ranging from anchoring or landing to controlling thrusters based on a position feedback from cameras or sonars systems. The former approach is not always feasible due to the lack of anchoring points or the type of substrate to land on, and the latter can only be achieved by actively controlling thrusters and does not guarantee perfect stillness, especially when the water is not clear or in the presence of current gusts. Moreover, even if perfect station keeping is achieved, pelagic robots are limited in exerting forces to the environment by the power of thrusters.

SILVER2 tackles these problems by being negatively buoyant and adopting a specific stance. In this way, station keeping can be simply achieved by holding motor positions and letting the friction with the ground passively reject the disturbance of the current. As shown in Fig. 3 and reported in Table 1, SILVER2 was capable of holding position with oscillations in the vertical position data of around 1.3 cm when subject to strong disturbances, absorbing an average of 1.56 A, which is slightly above the current absorbed by the electronic and control subsystems. A gross estimation of energetic autonomy (with the current on-board battery) allows monitoring operations for more than 16 hours.

In addition to that, SILVER2 presents a noise footprint completely different from traditional underwater robots. As mentioned earlier, when holding position, because no active disturbance rejection control is enforced, all motors are still, and thus, it is reasonable to claim that they do not make noise. On the other hand, when SILVER2 is hopping or walking, the typical noise footprint is reported in Fig. 7A, along with a recording of the noise when the robot is not moving. The noise footprints present patterns similar to the ones observed

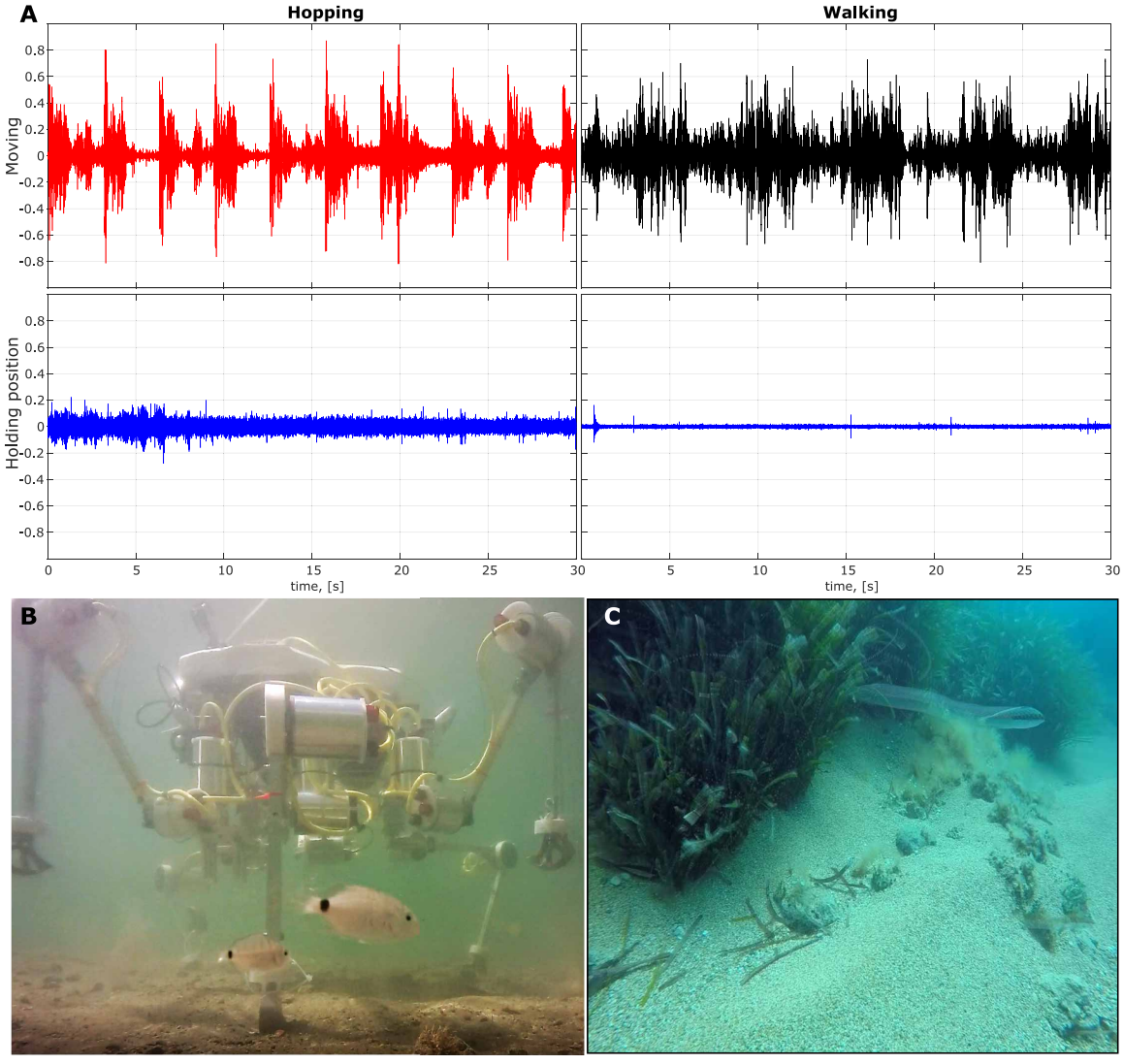

Fig. 7. Passive and noiseless station keeping. (**A**) Mp3 recordings of robot hopping, walking, and holding position. During holding position, motors are not active, so the signal is mostly noise from the surrounding environment. (**B**) Fish do not seem to be scared by the robot in motion. (**C**) Long exposure obtained from onboard cameras during station keeping.

in the current absorbed *c* (Fig. 3) because they are both connected with the activations of the motors. The noise footprint of hopping locomotion is periodic, with higher intensity during pushing and leg retractions, and is almost silent during swimming phases. On the other hand, the noise footprint of walking presents a higher mean value with lower peaks. The signal-to-noise ratio obtained from the signals shown in Fig. 7 resulted to be 13.05 and 25.48 dB for hopping and walking, respectively.

As final confirmation of low noise footprint, underwater fauna was not disturbed at all from the locomotion of the robot. Fishes moved alongside, ahead, and, occasionally, even among the legs (Fig. 7, B and C) of the robot. The unusual low noise footprint, combined with passive and reliable station keeping, allowed us to reconstruct long-exposure images from video collected: As shown in Fig. 7C, currents moved seaweed and sea snow, drawing white lines into the frame, while fishes passing by created a white shadow behind them. Conversely, static objects remain perfectly sharp, demonstrating the good passive stability of the robot.

DISCUSSION

Advantages of seabed vehicles were already clear, especially for high-force or long-time operations such as deep-sea mining and long-term monitoring (*39*). In particular, several studies attempted to quantify the impact of deep-sea mining and provide mitigation techniques to minimize the biodiversity loss [i.e., (*66*)]. However, at the time of writing, little was known about the impact and resilience of deep-sea mining on associated species (*67*). Furthermore, correct biological sampling and constant monitoring at regular intervals in time can only be achieved using vehicles that can explore the seabed using multiple ecological sensors, as pointed out by final users of underwater robots (*68*). Notwithstanding this, the use of state-of-the-art approaches for innovative locomotion (i.e., for legged robots)

has been unfeasible because it requires detailed knowledge of the surrounding environment (ground, obstacles, etc.), which is not available underwater. Therefore, seabed vehicles were traditionally developed around wheels or tracks, even though they carry all the drawbacks that motivated the research in legged robotics (*54*), plus additional difficulties imposed by the peculiar environment (*44*), which limit the use of seabed crawlers to specific seabed types.

The robot presented here overcomes such limitations with a bio-inspired approach to design and locomotion based on hopping. As shown in Fig. 4, SILVER2 successfully demonstrated hopping locomotion with little variability, as reported in Table 1, on different kinds of real underwater terrains even in the presence of slopes and without any previous information. In particular, we argue that crawlers such as the one in (*39*) would have probably been able to traverse seabed type S and R even though leaving a considerable footprint, but would have not been able to pass over big obstacles within the R ground, and could have tilting problems for the high dunes of ground D. ULRs using only static walking strategies, such as (*45*–*47*), would have probably had problems on seabed type D due to undulations of the ground and would have not been capable of passing an obstacle such as a rock.

Hopping and running locomotion have been extensively explored in the terrestrial environment, and experiments in controlled conditions revealed all its potential in terms of agility and ability to reject disturbances. However, performance inevitably degraded when robots are tested outside of the laboratory, and a high degree of context awareness and sophisticated control algorithms that go beyond simple mobility became necessary. The intrinsic characteristics of the underwater environment bring many advantages to the stability of legged locomotion, as was demonstrated in simulation in (*62*). In particular, the damping effect of hydrodynamic drag, the reduced weight due to buoyancy, and the stabilizing momentum generated by positioning the CoB above the CoM decrease the risk of falling and can be harnessed in the development and field use of ULRs.

The mean turning rate $\overline{\Psi}$, reported in Table 1, revealed that the poorest performance was obtained on seabed type R (silt and rocks) and the best on seabed type S (flat sand). Considering the seabed characteristics, a similar result was expected; however, it is worth remembering that the trials presented were obtained without any disturbance rejection control strategy or active control by the operator and lasted up to some minutes. For this reason, we consider the presented results as an excellent baseline performance on which the operator, a higher control hierarchy, and mechanical refinements will build upon.

Expected differences were found between the behavior of SILVER2 and the theoretical U-SLIP model as reported in the Supplementary Materials. In U-SLIP, the leg is assumed to be massless so that bringing it back in position when it is not in contact with the ground does not affect the locomotion dynamics. In SILVER2, legs have nonnegligible mass, and the retraction during swimming phases caused a negative peak in accelerations, which slowed down the robot and reduced the effect of rotations, as shown in Figs. 3 and 5D. Moreover, the robot is ballasted to be very light (around 150 g) underwater. This was done for multiple reasons including safety of operations, similarity with other underwater vehicles that are generally neutrally buoyant (or slightly positive), and to achieve higher hops to traverse irregular terrains. However, a heavier asset, as proved in simulations (*62*) and observed on a single-legged prototype (*64*), would decrease hopping height and increase frequency and horizontal speed. To prove the advantages of SILVER2, we did not use a buoyancy engine (to modulate the underwater weight of the robot) in this study, but it could have interesting implications on the control and asset regulation. For example, a heavier asset can be used in the presence of currents on a sandy substrate to be faster, whereas a lighter asset can be used in calm water on a very irregular terrain to hop over obstacles.

Our approach coped with uncertainties typical of underwater environments, such as disturbances of currents and limited sensing capabilities, together with uncertainties introduced by terrain irregularities, which is of great interest for delicate or complex substrates. Acceleration data demonstrated that robot-environment interaction could be controlled up to a certain extent. Different gaits produced different accelerations and therefore different forces. Gaits were not optimized to achieve a specific objective but rather to grant mobility and to demonstrate the raw capabilities of legged systems underwater. Although two gaits were presented, the potential of legged systems resides in the flexibility allowed by the legs themselves; thus, other strategies could be implemented to reduce the impact even more or to exert reaction forces in specific directions to cope with different tasks (manipulation, object collection, etc.). Furthermore, minimizing the acceleration signal during observation tasks—for example, by adopting a specific pose or gait to reject the disturbances of currents—might be an interesting control problem and an attractive feature for an underwater legged vehicle.

Scientific observations require disturbances to be limited as much as possible; moreover, there are specific situations where even a little displacement of sand will persist in water for several minutes (due to the fineness of sand), practically impairing observations in the disturbed area. This issue has strong implications for a mission's costs, and it makes landing systems, as well as landing maneuvers often performed by ROV pilots, practically useless. Although the presented gaits were not optimized, SILVER2 demonstrated both the delicateness required for long-time monitoring in such complex areas and the needed precise mobility.

Approaching a target could be dangerous for traditional underwater robots, when disturbances are particularly relevant. Especially in shallow water areas, robots are subject to waves that have substantial effect on their positioning capabilities. This is particularly relevant for small ROVs, which rarely have stabilization control. The omnidirectional walking gait of SILVER2 is specifically suited to safely approach a target and to get close without fear of accidental damage. The precise gait, coupled with the stability granted by legged system, allowed enough control to approach without concerns related to both environment and robot damage.

Moreover, the approaching procedure presented could be used to achieve high-quality bathymetry from an unusual perspective. Traditionally, bathymetric maps with photo rendering of the seabed can be obtained from AUVs by matching depth sensors, with laser measurements and possibly photographic images. State-of-the-art results have amazing resolution in the order of the millimeter in the direction tangential to the seabed, which degrade to the order of the centimeter in the direction orthogonal to the seabed (*30*). With our approach, we are in the opposite situation: Resolution is higher orthogonal to the seabed and lower tangentially. Possibly, by merging depth estimation, pose of the robot, and three-dimensional scenes reconstructed from stereo cameras, a high-quality bathymetry that integrates traditional bathymetric map in the direction orthogonal to the seabed could be obtained.

In addition, passive, inexpensive, and noiseless station keeping is a sought capability essentially enabled by being negatively buoyant and moving directly onto the seabed. SILVER2 demonstrated the ability of holding position with moderate, or even absent, oscillations in the vertical position (Fig. 3) without drifting or being dragged away by the current. Despite the low ballast, the station keeping was very effective, even allowing the reconstruction of long-exposure images (Fig. 7C). This confirms that the small oscillations observed from the pressure sensor during experiments were most probably caused by waves. In this context, SILVER2 provides a base upon which further biological studies on the current rejection strategies adopted by arthropods can be conducted. By designing a hydrodynamic carapace to reduce drag and lean to reject the disturbances by changing posture or exploiting anchoring, it is possible to further understand biological models and use SILVER2 as an experimental tool.

Moreover, SILVER2 demonstrated a noise footprint very different from traditional underwater vehicle, both when holding position and when moving, as shown in Fig. 7A. Thruster-propelled vehicles are very noisy; however, not much data are available in literature on their impact. The only alternatives are bioinspired robots, but the estimation of the noise is rarely available (to the authors' knowledge) with the exception of (*69*), which compares the noise footprint of an ROV and a bioinspired undulating robot. The estimation of the noise footprint of SILVER2 hereby presented is based on mp3 signals extracted from the mp4 recorded by a GoPro attached to the chassis of the robot (refer to the Supplementary Materials for the details); however, it is a good first-order approximation and provides a reference that is missing in literature. Moreover, a recording of pure environmental noise (when the robot is not present) is missing, but because the motors are not moving during station keeping tasks, we can reasonably consider the recordings during station keeping as such a reference. On the other hand, the same assumption could not be made for pelagic robots, which need continuous active compensation of thrusters to hold position.

The presented features are of direct interest for scientific observations. For example, low energetic costs and noise footprint during station keeping enable long-time, noninvasive monitoring of biota, but with the possibility of select point of view, pose, and other details not allowed by landing cameras. During the presented trials, fish appeared not to be afraid of the robot moving, as shown in Fig. 7B. In particular, the interaction between the emerging designs of legged underwater robots and underwater fauna is an interesting topic that could be explored in the future. Furthermore, the ability to be completely still facilitates the use of cameras and the post-processing of videos and images as demonstrated by the long exposition photo shown in Fig. 7C.

Despite the promises, practically ULRs presented so far (*17*, *45*, *46*, *70*) have not been regularly used in real applications either because of their massive size and deployment costs (*70*) or because of their nature of demonstrators (*17*) and, in all cases, because they exclusively use static locomotion strategies that do not perform well on irregular terrains with limited knowledge of the ground. Resorting to the bioinspired approach presented in this work can enhance their locomotion agility and increase their range of operations by the simple integration of compliant components in the legs and careful regulation of their underwater weight on the basis of U-SLIP simulations together with the implementation of the pushing control strategy hereby described. In addition, amphibious robots, which already integrate some form of compliancy in their paddle-like limbs (*57*, *58*), may implement and benefit from the underwater hopping strategy of SILVER2 through the integration of a subsystem that regulates their underwater weight to make them sink and the implementation of a pushing control strategy.

We consider the delicate and precise interaction, integrated with the ease of all-terrain locomotion and simplicity of control, as the strongest points of the legged approach proposed. Moreover, the long autonomy granted (16 hours of standing, 10 hours of hopping, and 7 hours of walking) on benthic realm and the noiseless characteristic of the robot open unexplored operational modalities difficult to match for pelagic robots. On the other hand, the limited mobility over long distances and the intrinsic limitation to work only onto the seabed constitute weak points that could not challenge the mobility of the traditional robots in the water column. The presented approach has specific advantages when a close interaction with the benthic realm is required for an extended period of time, and such benefits perfectly complement the drawbacks and difficulties of traditional underwater vehicles. ULRs represent an opportunity to exploit a difficult niche of underwater operations, with the potential of enhancing inspection, maintenance, and monitoring operations of resident (always kept in site) underwater systems. Obtaining similar performances (in terms of stability, positioning, energy consumption, and disturbance rejection) with algorithmic approaches on pelagic robots could scale back some advantages of the legged methodology, yet despite the great results and efforts performed so far by traditional robots, this objective appears still far from being realized. Moreover, intrinsic limitation (approximation of drag coefficient, movement of water to obtain motion, lag between actuation and action, etc.) of pelagic strategy may never allow to reach the performance of a ground system.

MATERIALS AND METHODS

System architecture

The overall system architecture is made of three nodes—i.e., SILVER2 robot, the operator, and a wireless buoy to connect them. SILVER2 (Fig. 2A) is a hexapod robot with segmented legs, each featuring three rotational degrees of freedom (DOFs) (namely, coxa, femur, and tibia joints; Fig. 2B) and a serial elastic on actuator implemented with two linear springs (k = 10 kN/m) on each tibia joint (Fig. 2D). The distal part of the leg (namely, foot; Fig. 2C) is equipped with a piezoelectric transducer used to sense touchdown and liftoff with the ground. The legs are actuated by an XM430-W350-R Dynamixel servomotor enclosed in aluminum canisters, sealed with O-rings to ensure waterproofing. The legs are attached to the chassis of the robot, which is made of two vertically arranged parallel polycarbonate plates, joined together by four horizontal aluminum bars and a Delrin plate to guarantee structural integrity to the vehicle and provide attachment points for two waterproof aluminum canisters lodging the power and the electronics and control subsystems. The power subsystem is made of a 12-V, 25,000-mA lithium battery, voltage and current sensors, a voltage regulator, and a power switch. The electronics and control subsystem consists of a main control unit (3.0 Raspberry Pi 3+) and sensors such as a pressure sensor (MS5837-30BA), inertial measurement units including three-axis magnetometer and embedded sensor fusion algorithm (BNO055), a custom board to read leakage sensors, and a custom board to read piezoelectric sensors. The robot is equipped with a camera subsystem made of a two-rotational DOF gimbal on which two high-definition cameras

are mounted to provide feedback to the user and enable stereoscopic vision and four dimmable torches. Last, the buoyancy subsystem is placed on the top part of the robot and is made of a single piece of incompressible foam and several anchoring points for smaller buoyant and ballasting elements to regulate the underwater asset of the robot according to environmental conditions.

The robot is remotely operated by a user through a graphic user interface that runs on a laptop and allows to select the locomotion mode, set control parameters, start and stop the locomotion, and perform sampling actions. The laptop of the operator is connected to a wireless antenna (Infinity Bullet M Omni) mounted on the buoy and connected to an Ethernet switch that is, in turn, connected directly to the Raspberry Pi on the robot through Ethernet cable.

Locomotion modes

SILVER2 is capable of two locomotion modes, i.e., hopping and walking. They are based on different control approaches and yield to locomotion features that can be harnessed in different tasks and contexts. The general idea was given in Results, whereas the following section deals with implementation details.

Hopping locomotion is based on two simple primitives, namely, extending and retracting, which, in turn, define two states in which each leg can be. A leg can be in the retracted position, closer to the body of the robot to guarantee ground clearance, or it can be in the extended position. These primitives are set by taking as a reference the dynamics of the U-SLIP model. For each leg, the two states are defined by the position of the coxa, femur, and tibia joint in that state. When the foot-ground contact is sensed, all legs are commanded to push, i.e., quickly move from the retracted position to the extended position. On the other hand, when the takeoff is detected, all legs are commanded to retract, i.e., transition from the extended to the retracted state. In case no touchdown/takeoff is detected for a long time, a timer triggers the extension/retraction primitive. The transition from the two states is obtained by simultaneously commanding the motors of the legs to reach the position of the next state. For each leg, the pushing action will generate a force applied on the leg attachment point on the chassis of the robot that depends on the retracted and extended states of the leg. The motion of the robot will result from the vector sum of the forces of the six legs. Depending on the relative positions of the legs, a momentum around a vertical axis could be generated, resulting in a rotation in place.

Walking locomotion is based on the inverse kinematics of the leg. For each foot, a closed trajectory in the leg frame is defined. The first part of the trajectory is a segment AB on the horizontal XY plane, corresponding to the contact phase. The second part of the trajectory is a hemi-ellipse in the plane defined by segment AB, corresponding to the swing phase. All legs follow the same trajectory with a phase lag. The robot will globally translate keeping its center of mass at constant height by a distance equal to the length of segment AB over the time that takes to complete the full trajectory, and the orientation of segment AB on the XY plane defines the overall direction of motion.

Sea trials

After about 4 hours of preliminary testing in a 2-m-deep pool, SILVER2 was deployed in the sea in four different locations ranging from a tourist marina with a shallow mixed seabed to a 12-m-deep open sea with sand and seaweed for a total of several hours. In each location, the robot was operated through visual feedback from the camera and commanded to perform walking and hopping with heuristic variations in the control parameters. During each action, there was no active steering by the operator. At the end of each trial, a set of data was extracted from the logging of sensors signals, and it was later analyzed as detailed in the Supplementary Materials.

For a more detailed description of subsystems, locomotion modes, and sea trials, including additional figures and the definitions of frames and variables, please refer to the Supplementary Materials.

SUPPLEMENTARY MATERIALS

robotics.sciencemag.org/cgi/content/full/5/42/eaaz1012/DC1
Text
Fig. S1. Exploded view of SILVER2 with all subsystems.
Fig. S2. CAD rendering of three-DOF segmented leg.
Fig. S3. Electronic subsystem.
Fig. S4. Exploded view of the camera canister.
Fig. S5. The original U-SLIP and the articulated version.
Fig. S6. Comparison between SILVER2 and U-SLIP simulation over a single step.
Fig. S7. Control of hopping locomotion.
Fig. S8. Parametric analysis of U-SLIP performance with respect to touchdown angle and spring stiffness.
Fig. S9. Control of omnidirectional walking locomotion.
Fig. S10 Reconstructed long-exposure images.
Table S1. Parameters of U-SLIP model and values used in simulations.
Table S2. Free parameters of omnidirectional walking gait.
Table S3. Data of the tests presented.
Movie S1. Hopping locomotion.
Movie S2. Hopping locomotion.
Movie S3. Walking locomotion.
Movie S4. Sea life.
Movie S5. Approaching procedure.

REFERENCES AND NOTES

1. G.-Z. Yang, J. Bellingham, H. Choset, P. Dario, P. Fischer, T. Fukuda, N. Jacobstein, B. Nelson, M. Veloso, J. Berg, Science for robotics and robotics for science. *Sci. Robot.* **1**, eaal2099 (2016).
2. M. Kovač, The bioinspiration design paradigm: A perspective for soft robotics. *Soft Robot.* **1**, 28–37 (2014).
3. P. Rolf, I. Fumiya, B. Josh, New robotics: Design principles for intelligent systems. *Artif. Life* **11**, 99–120 (2005).
4. C. Laschi, B. Mazzolai, M. Cianchetti, Soft robotics: Technologies and systems pushing the boundaries of robot abilities. *Sci. Robot.* **1**, 1–12 (2016).
5. D. W. Haldane, M. M. Plecnik, J. K. Yim, R. S. Fearing, Robotic vertical jumping agility via series-elastic power modulation. *Sci. Robot.* **1**, eaag2048 (2016).
6. A. M. Nasab, X. Huang, K. Kumar, M. K. Jawed, A. M. Nasab, Z. Ye, W. Shan, C. Majidi, Chasing biomimetic locomotion speeds: Creating untethered soft robots with shape memory alloy actuators. *Sci. Robot.* **3**, eaau7557 (2018).
7. K. Y. Ma, P. Chirarattananon, S. B. Fuller, R. J. Wood, Controlled flight of a biologically inspired, insect-scale robot. *Science* **340**, 603–607 (2013).
8. E. W. Hawkes, L. H. Blumenschein, J. D. Greer, A. M. Okamura, A soft robot that navigates its environment through growth. *Sci. Robot.* **2**, 1–8 (2017).
9. Y. Wang, X. Yang, Y. Chen, D. K. Wainwright, C. P. Kenaley, Z. Gong, Z. Liu, H. Liu, J. Guan, T. Wang, J. C. Weaver, R. J. Wood, L. Wen, A biorobotic adhesive disc for underwater hitchhiking inspired by the remora suckerfish. *Sci. Robot.* **2**, eaan8072 (2017).
10. O. M. Cliff, D. L. Saunders, R. Fitch, Robotic ecology: Tracking small dynamic animals with an autonomous aerial vehicle. *Sci. Robot.* **3**, eaat8409 (2018).
11. T. O. Fossum, G. M. Fragoso, E. J. Davies, J. E. Ullgren, R. Mendes, G. Johnsen, I. Ellingsen, J. Eidsvik, M. Ludvigsen, K. Rajan, Toward adaptive robotic sampling of phytoplankton in the coastal ocean. *Sci. Robot.* **4**, eaav3041 (2019).
12. N. Jacobstein, J. Bellingham, G.-Z. Yang, Robotics for space and marine sciences. *Sci. Robot.* **2**, eaan5594 (2017).
13. H. Singh, T. Maksym, J. Wilkinson, G. Williams, Inexpensive, small AUVs for studying ice-covered polar environments. *Sci. Robot.* **2**, eaan4809 (2017).

14. S. Chien, K. L. Wagstaff, Robotic space exploration agents. *Sci. Robot.* **2**, eaan4831 (2017).
15. J. G. Bellingham, K. Rajan, Robotics in remote and hostile environments. *Science* **318**, 1098–1102 (2007).
16. A. Ramezani, S.-J. Chung, S. Hutchinson, A biomimetic robotic platform to study flight specializations of bats. *Sci. Robot.* **2**, eaal2505 (2017).
17. J. Ayers, J. Witting, Biomimetic approaches to the control of underwater walking machines. *Philos. Trans. R. Soc. A Math. Phys. Eng. Sci.* **365**, 273–295 (2007).
18. R. K. Katzschmann, J. DelPreto, R. MacCurdy, D. Rus, Exploration of underwater life with an acoustically controlled soft robotic fish. *Sci. Robot.* **3**, eaar3449 (2018).
19. C. Deser, M. A. Alexander, S.-P. Xie, A. S. Phillips, Sea surface temperature variability: Patterns and mechanisms. *Annu. Rev. Mar. Sci.* **2**, 115–143 (2009).
20. G. R. Bigg, T. D. Jickells, P. S. Liss, T. J. Osborn, The role of the oceans in climate. *Int. J. Climatol.* **23**, 1127–1159 (2003).
21. J. S. Levinton, *Marine Biology: Function, Biodiversity, Ecology* (Oxford Univ. Press, 1995).
22. C. Alastair, *The Geography of Sea Transport* (Routledge, 2015).
23. M. E. McCormick, *Ocean Wave Energy Conversion* (Courier Corporation, 2013).
24. B. Snyder, M. J. Kaiser, Ecological and economic cost-benefit analysis of offshore wind energy. *Renew. Energy* **34**, 1567–1578 (2009).
25. I. L. White, K. E. Don, *Energy Under the Oceans: A Technology Assessment of Outer Continental Shelf Oil and Gas Operations* (The University of Oklahoma Press, 1973).
26. M. Quaas, J. Hoffman, K. Kamin, L. Kleemann, K. Schacht, *Fishing for Proteins* (WWF Germany; International WWF Centre for Marine Conservation, 2016).
27. G. Antonelli, *Underwater Robots* (Springer International Publishing, 2014).
28. A. Shukla, H. Karki, Application of robotics in onshore oil and gas industry-A review Part i. *Rob. Auton. Syst.* **75**, 490–507 (2016).
29. J. R. Martinez-de Dios, C. Serna, A. Ollero, Computer vision and robotics techniques in fish farms. *Robotica* **21**, 233–243 (2003).
30. M. Johnson-Roberson, M. Bryson, A. Friedman, O. Pizarro, G. Troni, P. Ozog, J. C. Henderson, High-resolution underwater robotic vision-based mapping and three-dimensional reconstruction for archaeology. *J. Field Robot.* **34**, 625–643 (2017).
31. Y.-W. Huang, Y. Sasaki, Y. Harakawa, E. F. Fukushima, S. Hirose, Operation of underwater rescue robot anchor diver III during the 2011 Tohoku Earthquake and Tsunami, in *OCEANS'11 MTS/IEEE KONA* (IEEE, 2011), pp. 1–6.
32. C. von Alt, B. Allen, T. Austin, N. Forrester, R. Goldsborough, M. Purcell, R. Stokey, Hunting for mines with REMUS: A high performance, affordable, free swimming underwater robot, in *MTS/IEEE Oceans 2001. An Ocean Odyssey* (IEEE, 2001), pp. 117–122.
33. J. Das, F. Py, J. B. J. Harvey, J. P. Ryan, A. Gellene, R. Graham, D. A. Caron, K. Rajan, G. S. Sukhatme, Data-driven robotic sampling for marine ecosystem monitoring. *Int. J. Robot. Res.* **34**, 1435–1452 (2015).
34. D. R. Yoerger, A. M. Bradley, B. B. Walden, M.-H. Cormier, W. B. F. Ryan, Fine-scale seafloor survey in rugged deep-ocean terrain with an autonomous robot, in *IEEE International Conference on Robotics and Automation* (IEEE, 2000), vol. 2, pp. 1787–1792.
35. O.-B. Humborstad, L. Nøttestad, S. Løkkeborg, H. T. Rapp, RoxAnn bottom classification system, sidescan sonar and video-sledge: Spatial resolution and their use in assessing trawling impacts. *ICES J. Mar. Sci.* **61**, 53–63 (2004).
36. M. Zhou, R. Bachmayer, B. deYoung, Mapping the underside of an iceberg with a modified underwater glider. *J. Field Robot.* **36**, 1102–1117 (2019).
37. Z. E. Teoh, B. T. Phillips, K. P. Becker, G. Whittredge, J. C. Weaver, C. Hoberman, D. F. Gruber, R. J. Wood, Rotary-actuated folding polyhedrons for midwater investigation of delicate marine organisms. *Sci. Robot.* **3**, eaat5276 (2018).
38. W. Martin, J. Baross, D. Kelley, M. J. Russell, Hydrothermal vents and the origin of life. *Nat. Rev. Microbiol.* **6**, 805–814 (2008).
39. C. Doya, D. Chatzievangelou, N. Bahamon, A. Purser, F. C. De Leo, S. K. Juniper, L. Thomsen, J. Aguzzi, Seasonal monitoring of deep-sea megabenthos in Barkley Canyon cold seep by internet operated vehicle (IOV). *PLOS ONE* **12**, e0176917 (2017).
40. N. A. Cruz, A. C. Matos, The MARES AUV, a modular autonomous robot for environment sampling, in *OCEANS 2008* (IEEE, 2008).
41. R. D. Christ, R. L. Wernli, *The ROV Manual: A User Guide for Remotely Operated Vehicles* (Elsevier, 2013).
42. D. Di Vito, G. Antonelli, The effect of the ocean current in the thrusters closed-loop performance for underwater intervention, in *OCEANS 2017 - Anchorage* (IEEE, 2017), pp. 1–6.
43. H. Yoshida, T. Aoki, H. Osawa, S. Ishibashi, Y. Watanabe, J. Tahara, T. Miyazaki, K. Itoh, A deepest depth ROV for sediment sampling and its sea trial result, in *2007 Symposium on Underwater Technology and Workshop on Scientific Use of Submarine Cables and Related Technologies* (IEEE, 2007), pp. 28–33.
44. T. Inoue, T. Shiosawa, K. Takagi, Dynamic analysis of motion of crawler-type remotely operated vehicles. *IEEE J. Ocean. Eng.* **38**, 375–382 (2013).
45. J. Akizono, T. Tanaka, K. Nakagawa, T. Tsuji, M. Iwasaki, Seabottom roughness measurement by aquatic walking robot, in *MTS/IEEE Conference Proceedings Oceans '97* (IEEE, 1997), pp. 1395–1398.
46. H. Greiner, A. Shectman, C. Won, R. Elsley, P. Beith, Autonomous legged underwater vehicles for near land warfare, in *Proceedings of Symposium on Autonomous Underwater Vehicle Technology* (IEEE, 1996), pp. 41–48.
47. B. H. Jun, H. Shim, J. Y. Park, B. Kim, P. M. Lee, A new concept and technologies of multi-legged underwater robot for high tidal current environment, in *2011 IEEE Symposium on Underwater Technology and Workshop on Scientific Use of Submarine Cables and Related Technologies* (IEEE, 2011), pp. 3–7.
48. S. Hirose, H. Kikuchi, Y. Umetani, The standard circular gait of a quadruped walking vehicle. *Adv. Robot.* **1**, 143–164 (1986).
49. R. Blickhan, R. J. Full, Similarity in multilegged locomotion: Bouncing like a monopode. *J. Comp. Physiol. A* **173**, 509–517 (1993).
50. R. Blickhan, The spring-mass model for running and hopping. *J. Biomech.* **22**, 1217–1227 (1989).
51. R. J. Full, D. E. Koditschek, Templates and anchors: Neuromechanical hypotheses of legged locomotion on land. *J. Exp. Biol.* **202**, 3325–3332 (1999).
52. M. Calisti, G. Picardi, C. Laschi, Fundamentals of soft robot locomotion. *J. R. Soc. Interface* **14**, 20170101 (2017).
53. R. Blickhan, A. Seyfarth, H. Geyer, S. Grimmer, H. Wagner, M. Günther, Intelligence by mechanics. *Philos. Trans. R. Soc. A Math. Phys. Eng. Sci.* **365**, 199–220 (2007).
54. M. H. Raibert, *Legged Robots That Balance* (MIT Press, 1986).
55. M. Raibert, BigDog, the rough-terrain quadruped robot 17, in *Proceedings of the 17th IFAC World Congress* (IFAC, 2008), vol. 17.
56. A. Spröwitz, A. Tuleu, M. Vespignani, M. Ajallooeian, E. Badri, A. J. Ijspeert, Towards dynamic trot gait locomotion: Design, control, and experiments with Cheetah-cub, a compliant quadruped robot. *Int. J. Robot. Res.* **32**, 932–950 (2013).
57. G. Dudek, P. Giguere, C. Prahacs, S. Saunderson, J. Sattar, L.-A. Torres-Mendez, M. Jenkin, A. German, A. Hogue, A. Ripsman, J. Zacher, E. Milios, H. Liu, P. Zhang, M. Buehler, C. Georgiades, AQUA: An amphibious autonomous robot. *Computer* **40**, 46–53 (2007).
58. A. R. Vogel, K. N. Kaipa, G. M. Krummel, H. A. Bruck, S. K. Gupta, Design of a compliance assisted quadrupedal amphibious robot, in *2014 IEEE International Conference on Robotics and Automation (ICRA)* (IEEE, 2014), pp. 2378–2383.
59. M. Calisti, F. Corucci, A. Arienti, C. Laschi, Dynamics of underwater legged locomotion: Modeling and experiments on an octopus-inspired robot. *Bioinspir. Biomim.* **10**, 046012 (2015).
60. M. M. Martinez, R. J. Full, M. A. Koehl, Underwater punting by an intertidal crab: A novel gait revealed by the kinematics of pedestrian locomotion in air versus water. *J. Exp. Biol.* **201**, 2609–2623 (1998).
61. M. Calisti, C. Laschi, Underwater running on uneven terrain, in *OCEANS 2015 - Genova* (IEEE, 2015), pp. 1–5.
62. M. Calisti, C. Laschi, Morphological and control criteria for self-stable underwater hopping. *Bioinspir. Biomim.* **13**, 016001 (2017).
63. M. Calisti, E. Falotico, C. Laschi, Hopping on uneven terrains with an underwater one-legged robot. *IEEE Robot. Autom. Lett.* **1**, 461–468 (2016).
64. G. Picardi, H. Hauser, C. Laschi, M. Calisti, Morphologically induced stability on an underwater legged robot with a deformable body. *Int. J. Robot. Res.*, 027836491984042 (2019).
65. G. Picardi, C. Laschi, M. Calisti, Model-based open loop control of a multigait legged underwater robot. *Mechatronics* **55**, 162–170 (2018).
66. K. A. Miller, K. F. Thompson, P. Johnston, D. Santillo, An overview of seabed mining including the current state of development, environmental impacts, and knowledge gaps. *Front. Mar. Sci.* **4**, 418 (2018).
67. S. Gollner, S. Kaiser, L. Menzel, D. O. B. Jones, A. Brown, N. C. Mestre, D. van Oevelen, L. Menot, A. Colaço, M. Canals, D. Cuvelier, J. M. Durden, A. Gebruk, G. A. Egho, M. Haeckel, Y. Marcon, L. Mevenkamp, T. Morato, C. K. Pham, A. Purser, A. Sanchez-Vidal, A. Vanreusel, A. Vink, P. Martinez Arbizu, Resilience of benthic deep-sea fauna to mining activities. *Mar. Environ. Res.* **129**, 76–101 (2017).
68. A. Brandt, J. Gutt, M. Hildebrandt, J. Pawlowski, J. Schwendner, T. Soltwedel, L. Thomsen, Cutting the Umbilical: New technological perspectives in benthic deep-sea research. *J. Mar. Sci. Eng.* **4**, 36 (2016).
69. K. Listewnik, Sound silencing problem of underwater vehicles. *Solid State Phenom.* **196**, 212–219 (2013).
70. B. H. Jun, P.-M. Lee, Y. Jung, Experience on underwater artefact search using underwater walking robot Crabster CR200, in *Oceans 2015 - MTS/IEEE Washington* (IEEE, 2015), pp. 1–5.

Acknowledgments: We thank the research assistant M. L. Macirella for work in design and development of the electrical and communication subsystem, as well as for invaluable support during missions. **Funding:** This research was partially funded by Arbi Dario S.p.A. under the framework of Blue Resolution project and by National Geographic Society under the framework of GOLD (Guardian of the Oceans Legged Drone) project, grant no. NGS-56544 T-19. **Author contributions:** G.P. and M. Calisti designed all experiments. M. Calisti, M. Chellapurath, and S.I. performed all the experiments. M. Calisti and C.L. conceptualized the ULR and bioinspired locomotion strategy. M. Calisti, M. Chellapurath, and S.I. designed and developed the ULR. G.P. designed and developed the software architecture, locomotion control, user interface, and software for the integration of electronics. M. Calisti, S.S., and C.L. were responsible for the overall research direction, objectives, and funding. M. Chellapurath and S.I. wrote part of the Supplementary Materials. G.P. and M. Calisti wrote the main text and the Supplementary Materials. **Competing interests:** The authors declare that they have no competing interests. **Data and materials availability:** All data needed to evaluate the conclusions in the paper are present in the paper or the Supplementary Materials.

Submitted 12 August 2019
Accepted 6 April 2020
Published 13 May 2020
10.1126/scirobotics.aaz1012

Citation: G. Picardi, M. Chellapurath, S. Iacoponi, S. Stefanni, C. Laschi, M. Calisti, Bioinspired underwater legged robot for seabed exploration with low environmental disturbance. *Sci. Robot.* **5**, eaaz1012 (2020).

Science Robotics

Bioinspired underwater legged robot for seabed exploration with low environmental disturbance

G. Picardi, M. Chellapurath, S. Iacoponi, S. Stefanni, C. Laschi, and M. Calisti

Sci. Robot. **5** (42), eaaz1012. DOI: 10.1126/scirobotics.aaz1012

Science Robotics (ISSN 2470-9476) is published by the American Association for the Advancement of Science. 1200 New York Avenue NW, Washington, DC 20005. The title *Science Robotics* is a registered trademark of AAAS.